griaule+1006

Griaule

Evaluation of Latent Friction Ridge Technology (ELFT)

Technical performance report of automated latent fingerprint feature extraction and search software.

Last Updated: 27 July 2022

Contents

Not Human Subjects Research
The National Institute of Standards and Technology's Research Protections Office reviewed the protocol for this project and determined it is "not human subjects research" as defined in 15 CFR 27, the Common Rule for the Protection of Human Subjects.

Disclaimer
Certain commercial entities, equipment, or materials may be identified in this document in order to describe an experimental procedure or concept adequately. Such identification is not intended to imply recommendation or endorsement by the National Institute of Standards and Technology, nor is it intended to imply that the entities, materials, or equipment are necessarily the best available for the purpose.

NATIONAL INSTITUTE OF STANDARDS AND TECHNOLOGY
U.S. DEPARTMENT OF COMMERCE

1 Participation Information

1.1 Names

Information in this section is provided by the participant.

- **Participant Name:** Griaule
- **ELFT Identifier:** griaule+1006
- **Exemplar Feature Extractor:**
  - **Marketing Name:** Griaule Implementation Exemplar Extractor 1.0
  - **CBEFF Product Owner:** 0x003A
  - **CBEFF Algorithm Identifier:** 0x01A7
- **Latent Feature Extractor:**
  - **Marketing Name:** Griaule Implementation Latent Extractor 1.0
  - **CBEFF Product Owner:** 0x003A
  - **CBEFF Algorithm Identifier:** 0x01AC
- **Search:**
  - **Marketing Name:** GriauleImplementation Matcher 1.0
  - **CBEFF Product Owner:** 0x003A
  - **CBEFF Algorithm Identifier:** 0x0101

1.2 Dates

- **Application Date:** 06 June 2021
- **First Submission Date:** 26 November 2021 (as version 1001)
- **Final Submission Date:** 01 March 2022 (as version 1006)
- **Validation Date:** 02 March 2022
- **Completion Date:** 29 April 2022
- **Report Last Updated Date:** 27 July 2022

1.3 Supplied Libraries and Configurations

Testing completed using Ubuntu 20.04.3 LTS.

Table 1: Information regarding library and configuration files provided as part of griaule+1006.

Filename	MD5 Checksum	Size (MB)
libonnxruntime.so	8bb7a46fb9b4f9dc214d44a2a8e78d70	12.7
libelft_griaule_1006.so	94562aa7fd024a2c650a0783ae7f2557	31.9

2 Timing Sample

A fixed sample of images was randomly and proportionally selected from the ELFT datasets in 2021. The sample is used to assess whether an implementation adheres to the computational speed requirements from the ELFT Test Plan. These values are chosen in such a way that allows the implementation flexibility while allowing NIST to complete the evaluation in a reasonable amount of time. If an implementation exceeds the maximum allowable duration, the participant will be asked to reduce the processing time of their software prior to NIST completing the evaluation. As such, *all* published ELFT submissions conform to the published speed requirements.

2.1 Processor Details

All measurements in this section were performed on a machine equipped with Intel Xeon Gold 6254 Central Processing Units (CPUs). Each CPU features a 3.10 GHz base frequency and 24.75 MB of cache. Timing tests are all **single threaded**—implementations are not permitted to use more than one thread during any function measured here. As such, these values can be used to understand expected scaled performance. NIST testing code embraces the single-threaded nature of implementations to `fork` processes during other non-timed portions of this evaluation, allowing participants to write thread-unsafe code while still using NIST resources to their maximum efficiency. This CPU supports executing several families of processor intrinsic functions, including AVX-512[1].

2.2 Composition

Table 2 shows the quantity of each type of fingerprint image comprising the timing sample dataset.

Table 2: Number of images of each generalized finger position comprising the timing sample dataset.

Image Type	Quantity
Latent	250
Four Finger	476
Full Palm	40
Partial Palm	47
Single Finger	2 784

2.3 Feature Extraction

Features were extracted from all images depicted in Table 2 and stored in templates. If a sample contained EFS data, it was included during this test.

2.3.1 Template Size

Table 3 and Figure 1 show the distribution of file sizes of templates. Failures of any kind reported during template generation result in NIST code writing 0 byte files. These files are excluded from the template size analysis in this section.

[1]The complete set of advertised CPU flags is `fpu`, `vme`, `de`, `pse`, `tsc`, `msr`, `pae`, `mce`, `cx8`, `apic`, `sep`, `mtrr`, `pge`, `mca`, `cmov`, `pat`, `pse36`, `clflush`, `dts`, `acpi`, `mmx`, `fxsr`, `sse`, `sse2`, `ss`, `ht`, `tm`, `pbe`, `syscall`, `nx`, `pdpe1gb`, `rdtscp`, `lm`, `constant_tsc`, `art`, `arch_perfmon`, `pebs`, `bts`, `rep_good`, `nopl`, `xtopology`, `nonstop_tsc`, `cpuid`, `aperfmperf`, `pni`, `pclmulqdq`, `dtes64`, `monitor`, `ds_cpl`, `vmx`, `smx`, `est`, `tm2`, `ssse3`, `sdbg`, `fma`, `cx16`, `xtpr`, `pdcm`, `pcid`, `dca`, `sse4_1`, `sse4_2`, `x2apic`, `movbe`, `popcnt`, `tsc_deadline_timer`, `aes`, `xsave`, `avx`, `f16c`, `rdrand`, `lahf_lm`, `abm`, `3dnowprefetch`, `cpuid_fault`, `epb`, `cat_l3`, `cdp_l3`, `invpcid_single`, `intel_ppin`, `ssbd`, `mba`, `ibrs`, `ibpb`, `stibp`, `ibrs_enhanced`, `tpr_shadow`, `vnmi`, `flexpriority`, `ept`, `vpid`, `ept_ad`, `fsgsbase`, `tsc_adjust`, `bmi1`, `avx2`, `smep`, `bmi2`, `erms`, `invpcid`, `cqm`, `mpx`, `rdt_a`, `avx512f`, `avx512dq`, `rdseed`, `adx`, `smap`, `clflushopt`, `clwb`, `intel_pt`, `avx512cd`, `avx512bw`, `avx512vl`, `xsaveopt`, `xsavec`, `xgetbv1`, `xsaves`, `cqm_llc`, `cqm_occup_llc`, `cqm_mbm_total`, `cqm_mbm_local`, `dtherm`, `ida`, `arat`, `pln`, `pts`, `pku`, `ospke`, `avx512_vnni`, `md_clear`, `flush_l1d`, `arch_capabilities`

Table 3: Template file size summary statistics as seen on the Timing Sample dataset, in kB.

Image Type	Minimum	25%	Median	Mean	75%	Maximum	Failures	Attempts
Latent	2.7	7.2	9.9	14.2	14.5	196.3	7	250
Single Finger	0.3	10.9	13.8	14.1	17.3	27.9	0	2 784
Four Finger	5.2	17.9	21.1	21.2	24.3	40.4	0	476
Partial Palm	0.1	67.4	91.5	95.1	112.9	302.4	0	47
Full Palm	240.5	274.5	321.4	322.2	353.3	450.7	0	40

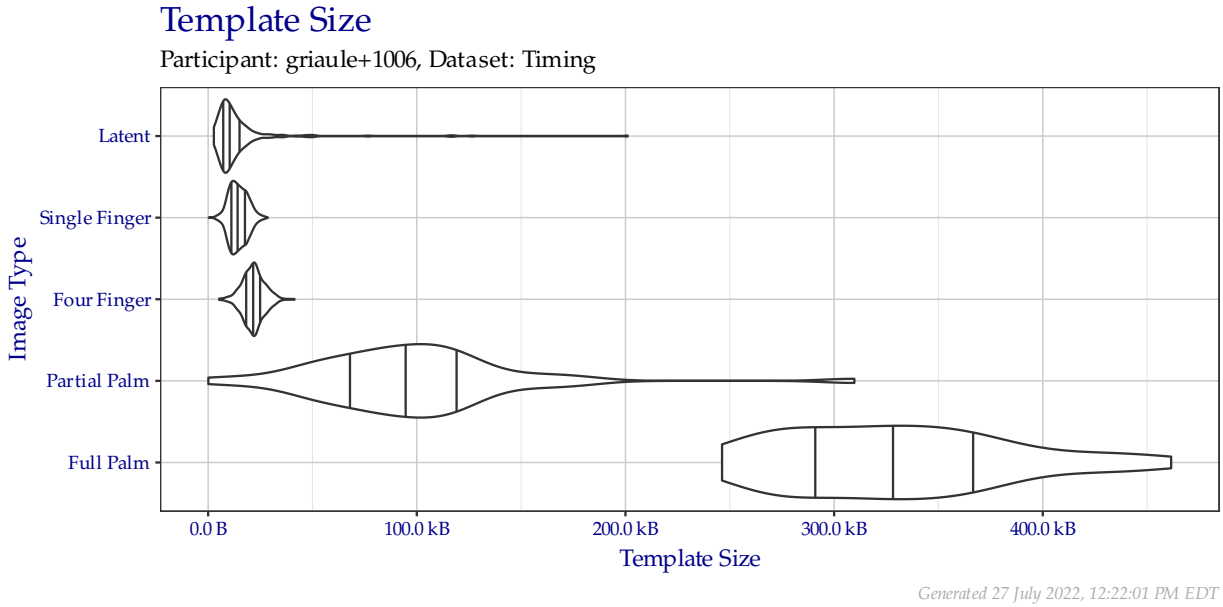

Figure 1: Violin plot of template file sizes as seen on the Timing Sample dataset. Vertical lines from left to right indicate the 25%, 50%, and 75% quantiles respectively.

2.3.2 Template Creation Duration

Table 4 and Figure 2 show the distribution template creation durations in seconds. Failures of any kind reported during template generation result in NIST code writing 0 byte files, but only after the template creation method returns. These times are excluded in the template creation duration analysis in this section.

Table 4: Duration of template creation in seconds for images from the Timing Sample dataset.

Image Type	Minimum	25%	Median	Mean	75%	Maximum	Failures	Attempts
Latent	0.3	1.6	2.2	3.1	3.2	31.6	7	250
Single Finger	0.1	0.7	0.8	0.8	0.9	1.2	0	2 784
Four Finger	0.2	0.6	0.7	0.7	0.8	1.8	0	476
Partial Palm	2.0	3.7	4.7	4.8	5.3	19.4	0	47
Full Palm	10.6	11.6	12.3	12.7	13.5	17.1	0	40

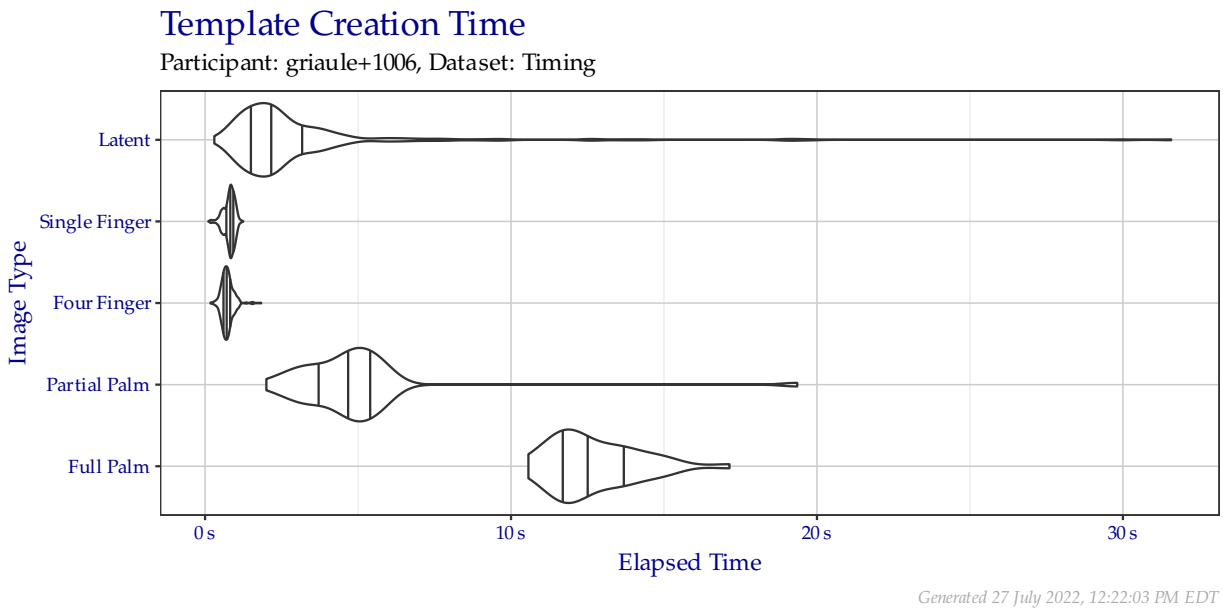

Figure 2: Violin plot of the duration of template creation in seconds for images from the Timing Sample dataset. Vertical lines from left to right indicate the 25%, 50%, and 75% quantiles respectively.

2.3.3 Template Creation Memory Consumption

Figure 3 shows the amount of RAM consumed by the single testing process as a function of time during the template creation procedure, including RAM consumed by the NIST testing apparatus.

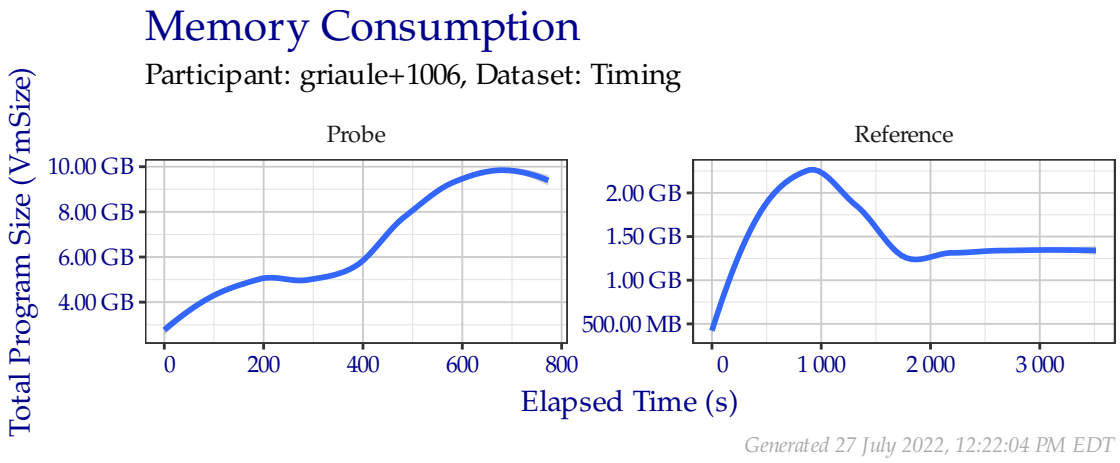

Figure 3: Amount of RAM used while creating templates in the Timing Sample dataset.

2.4 Enrollment Database

Reference templates are combined into a participant-defined database structure for optimal searching. The required storage for the Timing Sample enrollment database with plain impression distractors was **105.8 GB** and the required storage for the Timing Sample enrollment database with rolled impression distractors was **251.1 GB**.

2.5 Search

Out of the latent templates generated in Table 2, a fixed random sample of 100 of the resulting latent templates were searched against an enrollment set of ≈ 1 600 000 non-mated images. The results presented in Subsection 2.5 are based on the measurements made on or during those 100 searches.

2.5.1 Search Duration

Table 5 and Figure 4 show the amount of time elapsed during searches of the fixed search probe set when searching against enrollment sets of ≈ 1 600 000 non-mated images. While unsuccessful searches expend operator time, they are not included in this metric, because search failures typically occur instantaneously (e.g., a template indicates that that a probe was of too poor quality to search), which can artificially lower the average search time.

Table 5: Search time durations of the search probe set from the Timing Sample dataset, in seconds.

Distractor Imp.	Mated?	Min	25%	Median	Mean	75%	Maximum	Failures	Searches
Plain	False	60	467	937	1 539	1 987	6 474	7	100
Plain	True	149	1 412	2 693	3 915	5 695	13 563	7	100
Roll	False	154	1 409	2 703	3 910	5 737	13 585	7	100
Roll	True	145	1 408	2 681	3 898	5 689	13 519	7	100

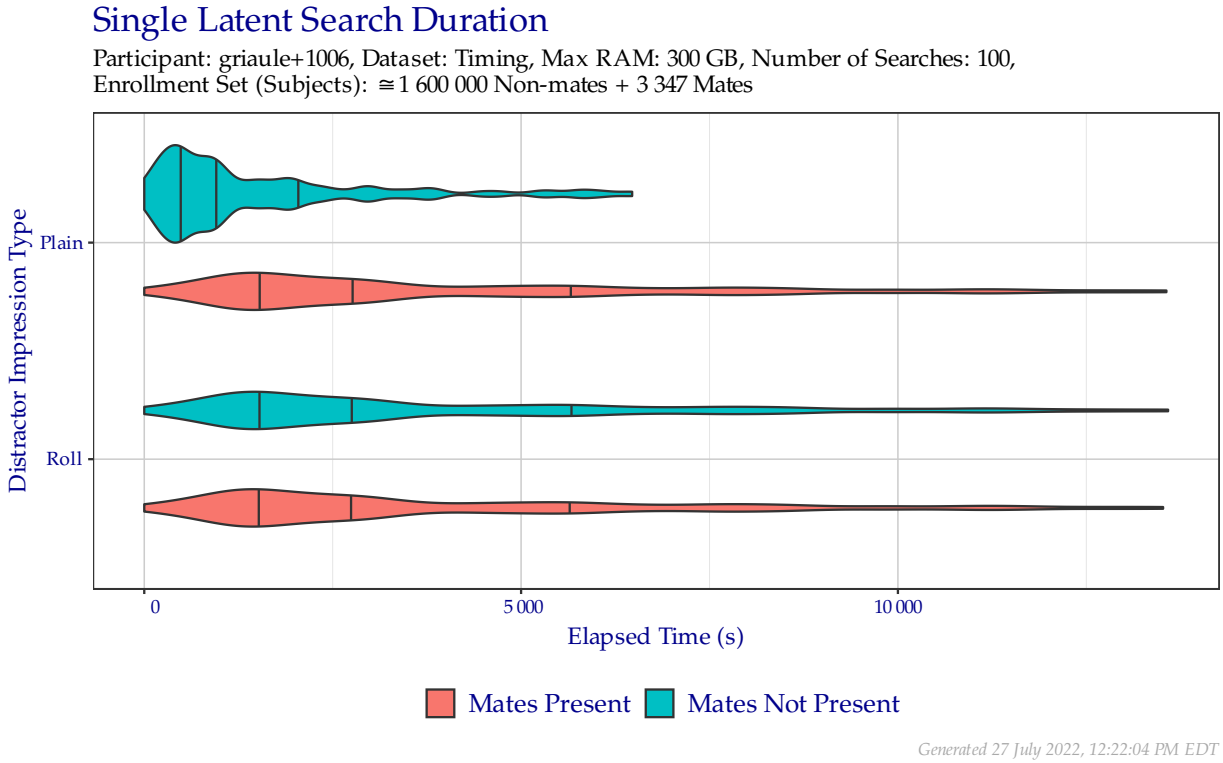

Figure 4: Violin plot of search time durations of the search probe set from the Timing Sample dataset. Vertical lines from left to right indicate the 25%, 50%, and 75% quantiles respectively.

2.5.2 Search Memory Consumption

Figure 5 shows the amount of RAM consumed by the single testing process as a function of time during the search procedure, including RAM consumed by the NIST testing apparatus. Implementations were permitted to use up to 300 GB to store templates. Note the different scales on each panel—implementations that do not change the contents of RAM may not show variation.

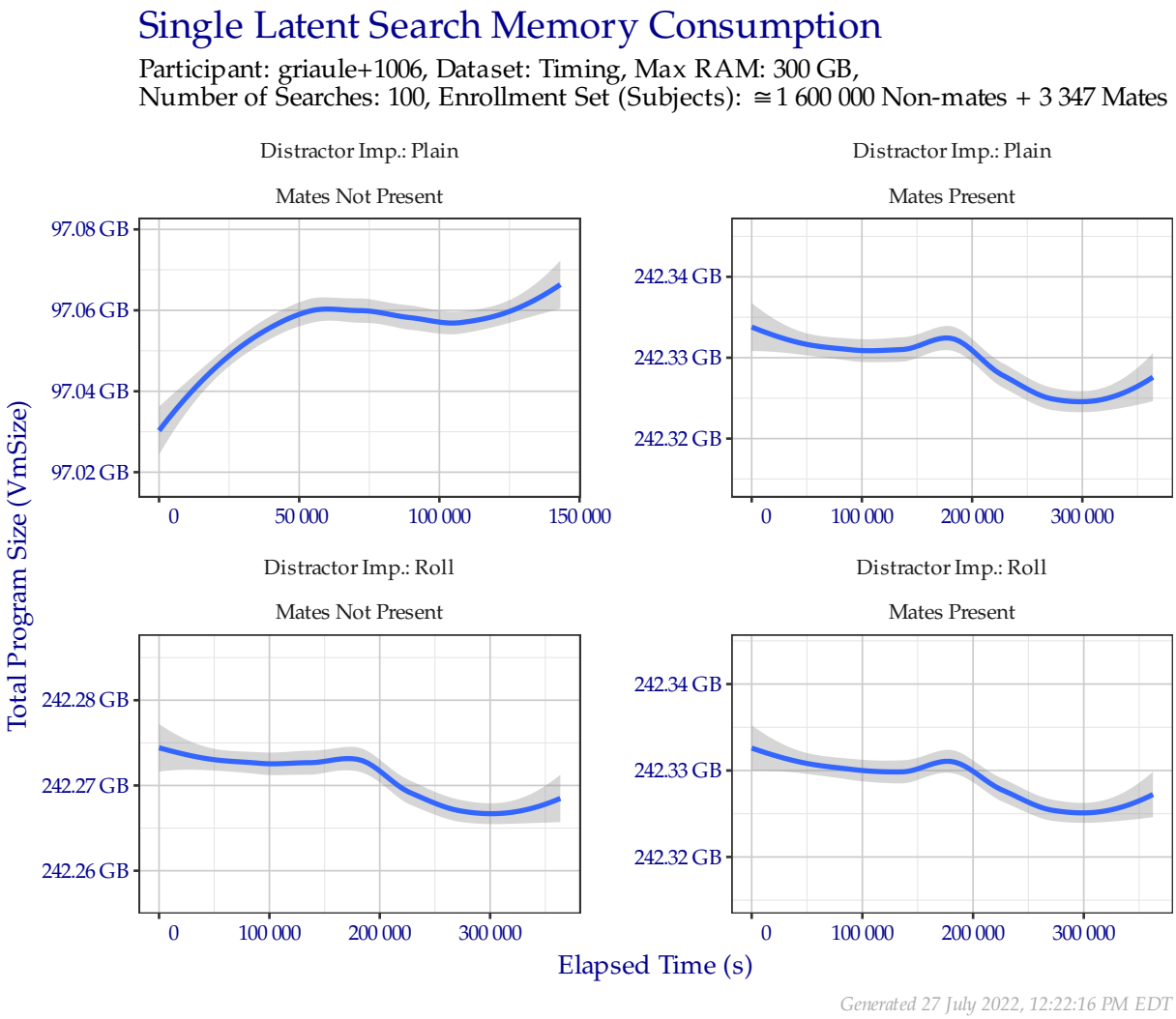

Figure 5: Amount of RAM used while searching templates in the Timing Sample dataset.

3 Metrics

3.1 Location

When a metric depicts search accuracy in this document, it is reported in terms of Location: Region, Hand, and Subject.

- **Region**: The correct region of the correct subject was returned.
  - For search probes sourced from a distal phalanx (i.e., a "latent fingerprint"), the correct finger position 1–10 shall be returned.
  - For search probes sourced from a palm or a non-distal phalanx, the most localized region shall be returned. Some palm regions may be interchangeable based on the exemplars provided (e.g., a palm probe's source could reasonably be seen in a lower palm, hypothenar, and writer's palm exemplar). Credit is given for **Region** in this case.
- **Hand**: A friction ridge position from anywhere on the correct hand of the correct subject is returned. This is designed to aid in diagnosing segmentation error.
- **Subject**: Any finger position from the correct subject is returned. This is designed to reward the situation where an implementation cannot ascertain the most localized region from the set of exemplars enrolled.

3.2 Cumulative Match Characteristic (CMC)

The Cumulative Match Characteristic (CMC) plots in this document show the false negative identification rate (FNIR) without respect for similarity score when searching probes against a enrollment database where a single mated identity for each search probe was present.

- ≈ 1 600 000 non-mated subjects were enrolled.
  - All subjects had at least one, but typically ten, distal phalanx captures to enroll. ≈ 150 000 had one or more palm captures to enroll.
  - Two different combinations of non-mates were searched in separate enrollment databases. While both contain the identical subjects, one set contains only plain impressions and the other contains only rolled impressions.
- The requested size of the candidate list was always 100 subjects.
- All possible Extended Feature Set (EFS) data was provided when "Image + EFS" is listed for probes. The type of EFS data present varies for each sample in each dataset. Initial experiments show nominal (if any) change when EFS data was provided alongside exemplars.
- Probe impression type was always "Unknown Finger" or "Unknown Palm," as appropriate. Future studies may show results using the impression type "Unknown Friction Ridge" for both types of probes.
- The metric *hit rate* is equivalent to 1 − miss rate, or 1 − FNIR. For example, an FNIR of 0.1 indicates a hit rate of 0.9 (i.e., 90%).

3.3 Detection Error Tradeoff (DET)

The Detection Error Tradeoff (DET) plots in this document show the tradeoff between false positive and false negative identification rates when searching probes against a enrollment database where a single mated identity for each search probe was present.

- ≈ 1 600 000 non-mated subjects were enrolled.
  - All subjects had at least one, but typically ten, distal phalanx captures to enroll. ≈ 150 000 had one or more palm captures to enroll.
  - Two different combinations of non-mates were searched in separate enrollment databases. While both contain the identical subjects, one set contains only plain impressions and the other contains only rolled impressions.
  - Non-mated similarity scores come from all ranks when searching probes against an enrollment dataset without any mated subjects enrolled.
- The requested size of the candidate list was always 100 subjects.

  - Mated similarity scores come from the correct location appearing at *any* rank.
- All possible EFS data was provided when "Image + EFS" is listed for probes. The type of EFS data present varies for each sample in each dataset. Initial experiments show nominal (if any) change when EFS data was provided alongside exemplars.
- Probe impression type was always "Unknown Finger" or "Unknown Palm," as appropriate. Future studies may show results using the impression type "Unknown Friction Ridge" for both types of probes.

4 Non-mated Distractor Subjects

When searching probes in each of the subsequent sections, the non-mated distractor subjects that comprised the majority of each enrollment database remained the same. The results of Section 4 are based off of these distractor subjects.

4.1 Failures

Table 6 shows the number of failures to create reference templates for non-mated distractor subjects.

Table 6: Number of failures to create reference templates.

Distal Phalanx Impression Type	Failures	≈ Attempts
Plain	0	1 600 000
Roll	0	1 600 000

5 FBI Laboratory

The results of Section 5 are based on searches of the sequestered dataset *FBI Laboratory*. This dataset consists of 49 operational latent distal phalanx probes. Members of the FBI manually annotated the probe images and confirmed the ground truth mate. EFS data provided with the probe image includes minutia locations provided by the FBI. All probes searched were a single sample depicting a region from a distal phalanx.

5.1 Failures

Table 7 shows the number of failures to create templates. Table 8 shows the number of failures to produce a candidate list.

Table 7: Number of failures to create templates.

Image Type	Content	Failures	Attempts
Exemplar	Image	0	38
Probe	Image + EFS	0	49
Probe	Image	0	49

Table 8: Number of failures to produce a candidate list. This number includes any failures to create a probe template from Table 7.

Distractor Imp.	Probe Content	Failures	Attempts
Plain	Image	0	49
Roll	Image	0	49
Plain	Image + EFS	0	49
Roll	Image + EFS	0	49

5.2 CMC Plots

The CMC plots in Figure 6 show the FNIR of griaule+1006 when searching FBI Laboratory against enrollment database where a single mated identity for each search probe was present. The plots are faceted by the distractor impression type and whether probe EFS data was provided. Tabular versions of FNIR at select ranks can be viewed in Table 9.

5.3 CMC Table

The values in Table 9 correspond to Figure 6.

Table 9: Region FNIR values from CMC plotted in Figures 6.

Distractor Imp.	Probe Content	Rank 1	Rank ≤ 50	Rank ≤ 100
Plain	Image	0.3265	0.2857	0.2653
Roll	Image	0.3265	0.2857	0.2653
Plain	Image + EFS	0.3265	0.2857	0.2857
Roll	Image + EFS	0.3265	0.2857	0.2857

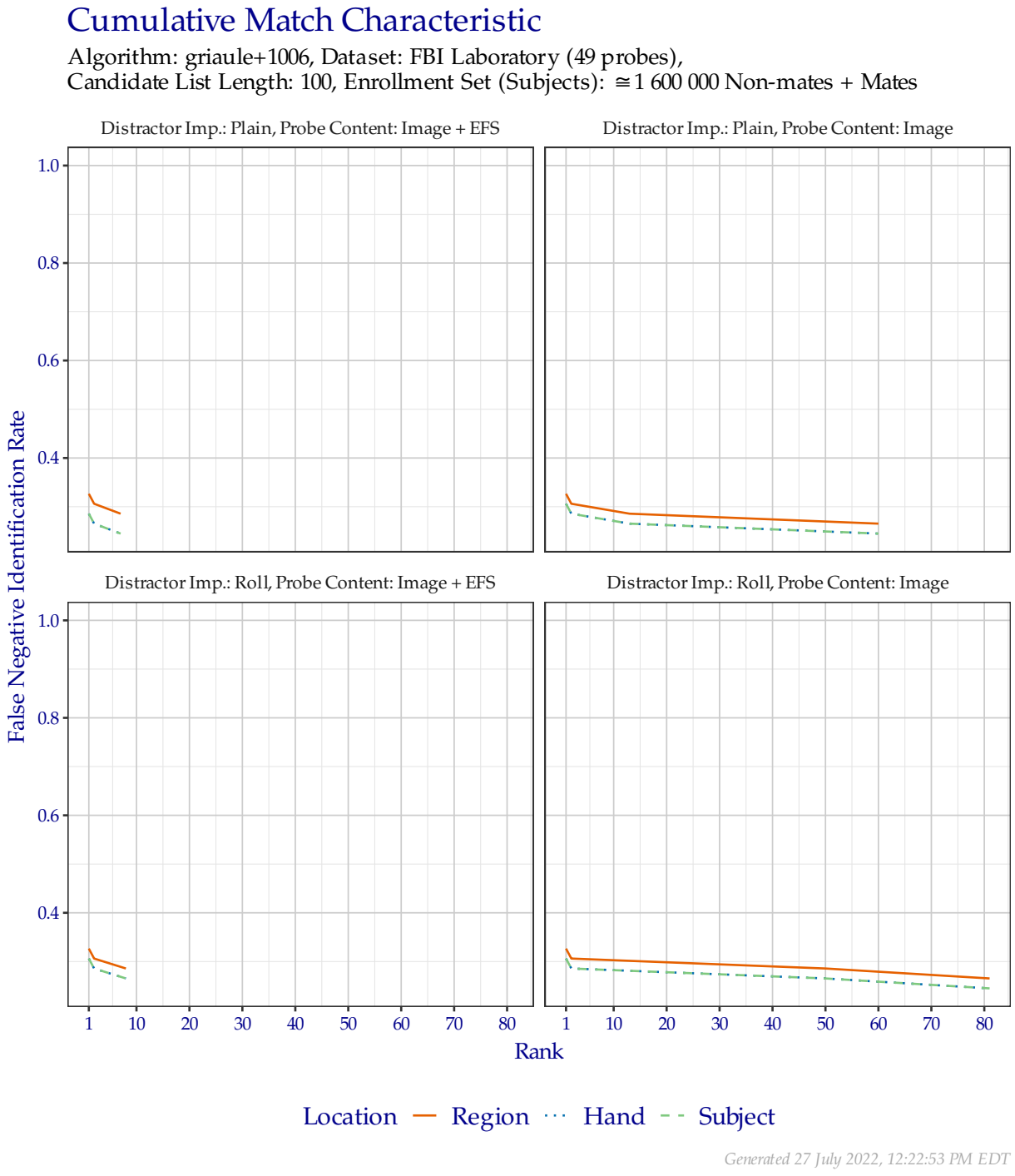

Figure 6: CMC when searching FBI Laboratory probes, faceted by distractor impression type and whether probe EFS data was provided.

5.4 DET Plots

The DET plots in Figure 7 show the false positive and false negative identification rate tradeoffs of griaule+1006 when searching FBI Laboratory against enrollment database where a single mated identity for each search probe was present. The plots are faceted by the distractor impression type and whether probe EFS data was provided. Tabular versions of FNIR at select FPIR can be viewed in Table 10.

5.5 DET Table

The values in Table 10 correspond to Figure 7.

Table 10: Region FNIR values corresponding to FPIR plotted in Figure 7.

Distractor Imp.	Probe Content	FPIR = 0.01	FPIR = 0.02	FPIR = 0.1
Plain	Image	0.2222	0.1944	0.1389
Roll	Image	0.2778	0.2222	0.1667
Plain	Image + EFS	0.1143	0.0857	0.0571
Roll	Image + EFS	0.2571	0.1429	0.0571

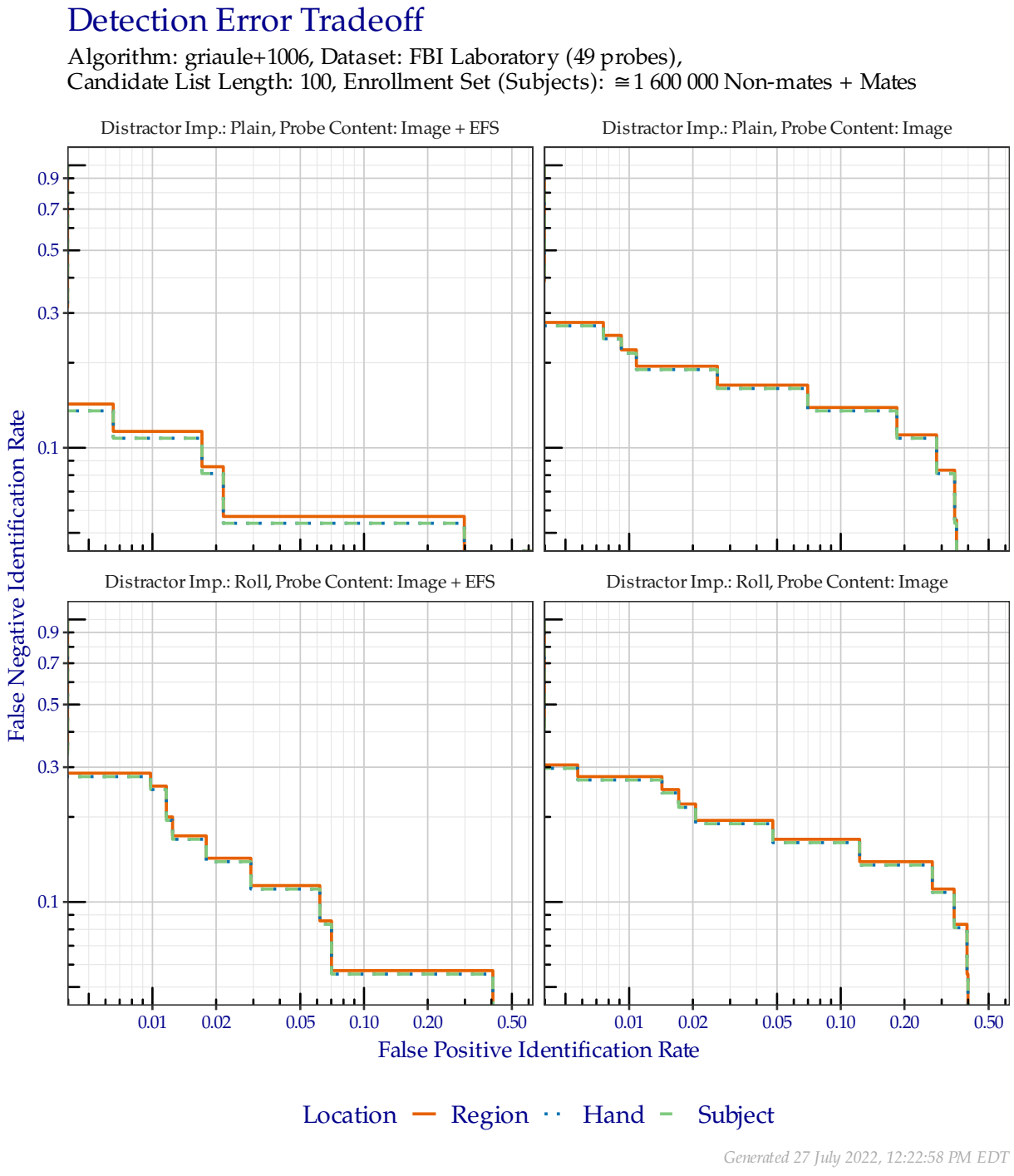

Figure 7: DET when searching FBI Laboratory probes, faceted by the distractor impression type and whether probe EFS data was provided.

6 FBI-Provided Solved Dataset #1

The results of Section 6 are based on searches of the sequestered dataset *FBI-Provided Solved Dataset #1*. This dataset consists of 516 operational probes collected from a particular type of crime. Members of the FBI manually annotated the probe images and confirmed the ground truth mate. EFS data provided with the probe image includes minutia locations provided by the FBI. All probes searched were a single sample depicting a region from a distal phalanx.

6.1 Failures

Table 11 shows the number of failures to create templates. Table 12 shows the number of failures to produce a candidate list.

Table 11: Number of failures to create templates.

Image Type	Content	Failures	Attempts
Exemplar	Image	0	173
Probe	Image + EFS	1	516
Probe	Image	1	516

Table 12: Number of failures to produce a candidate list. This number includes any failures to create a probe template from Table 11.

Distractor Imp.	Probe Content	Failures	Attempts
Plain	Image	1	516
Roll	Image	1	516
Plain	Image + EFS	1	516
Roll	Image + EFS	1	516

6.2 CMC Plots

The CMC plots in Figure 8 show the FNIR of griaule+1006 when searching FBI-Provided Solved Dataset 1 against enrollment database where a single mated identity for each search probe was present. The plots are faceted by the distractor impression type, mated impression type, and whether probe EFS data was provided. Tabular versions of FNIR at select ranks can be viewed in Table 13.

6.3 CMC Table

The values in Table 13 correspond to Figure 8.

Table 13: Region FNIR values from CMC plotted in Figure 8.

Distractor Imp.	Probe Content	Rank 1	Rank $\leq$ 50	Rank $\leq$ 100
Plain	Image	0.3915	0.3023	0.2849
Roll	Image	0.3953	0.3062	0.2946
Plain	Image + EFS	0.3740	0.2829	0.2674
Roll	Image + EFS	0.3760	0.2907	0.2810

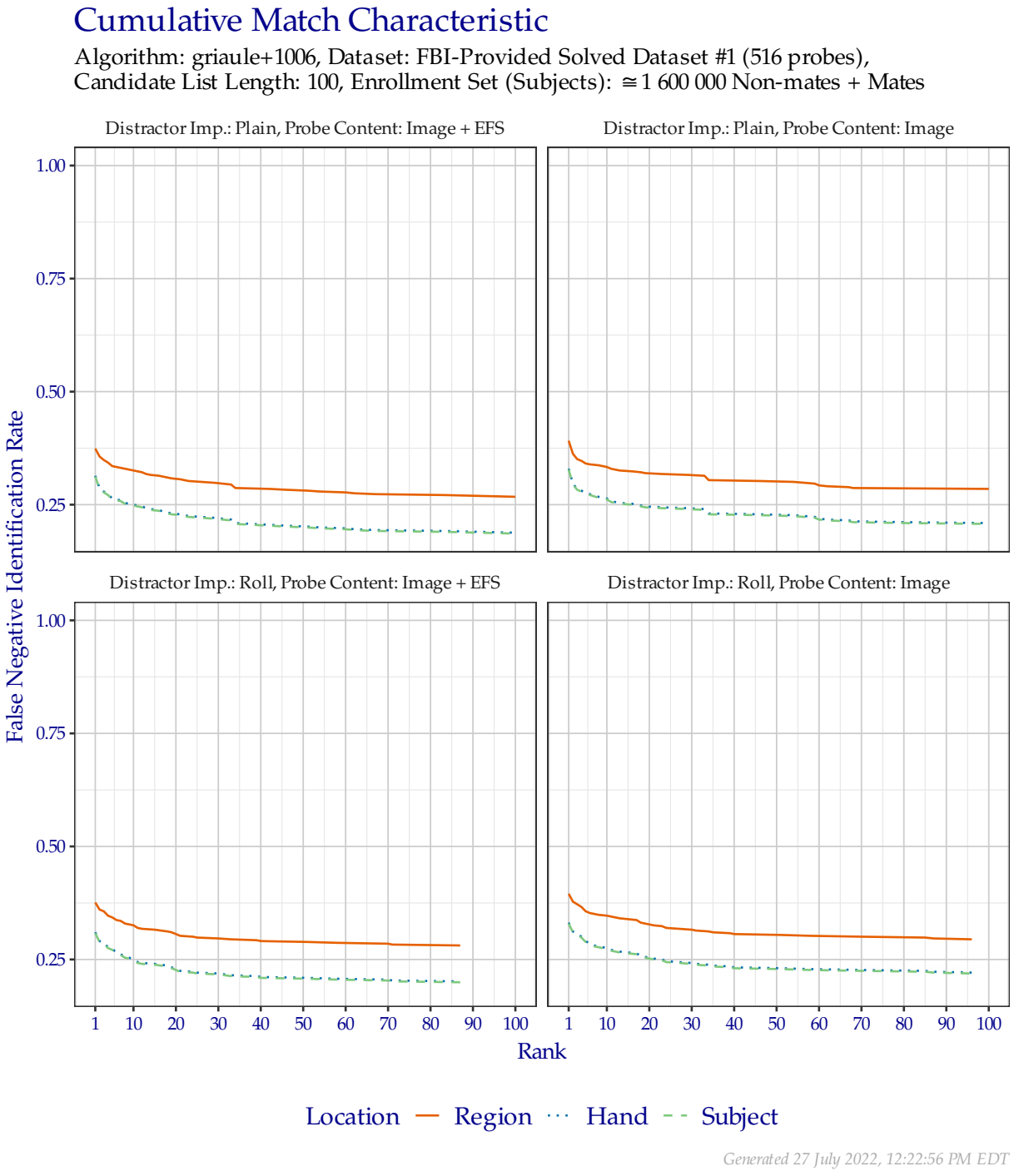

Figure 8: CMC when searching FBI-Provided Solved Dataset 1 probes, faceted by distractor impression type, mated impression type, and whether probe EFS data was provided.

6.4 DET Plots

The DET plots in Figure 9 show the false positive and false negative identification rate tradeoffs of griaule+1006 when searching FBI-Provided Solved Dataset 1 against enrollment database where a single mated identity for each search probe was present. The plots are faceted by the distractor impression type, mated impression type, and whether probe EFS data was provided. Tabular versions of FNIR at select FPIR can be viewed in Table 14.

6.5 DET Table

The values in Table 14 correspond to Figure 9.

Table 14: Region FNIR values corresponding to FPIR plotted in Figure 9.

Distractor Imp.	Probe Content	FPIR = 0.01	FPIR = 0.02	FPIR = 0.1
Plain	Image	0.3767	0.3523	0.2358
Roll	Image	0.3874	0.3626	0.2363
Plain	Image + EFS	0.4180	0.3704	0.2143
Roll	Image + EFS	0.4151	0.3639	0.2210

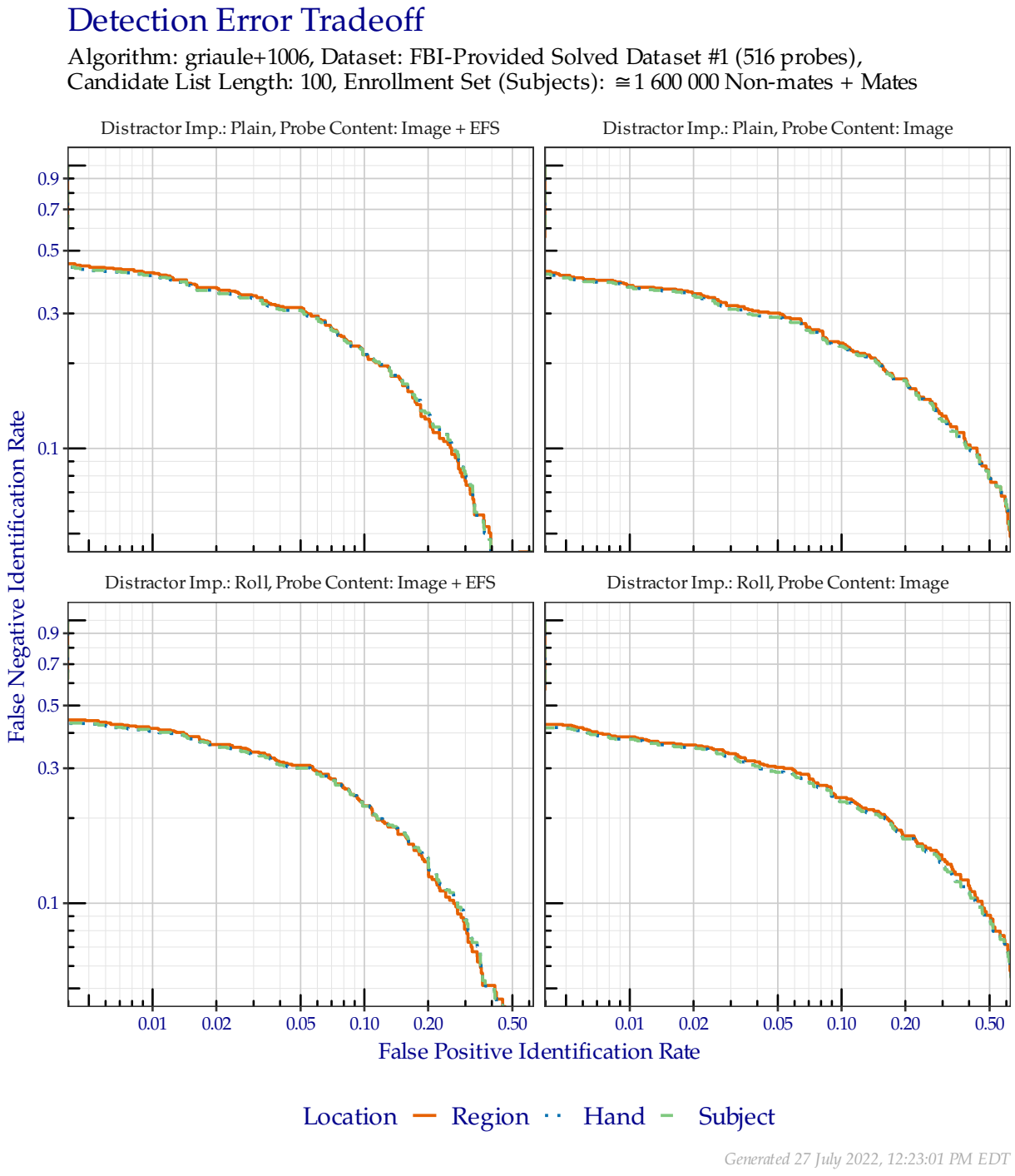

Figure 9: DET when searching FBI-Provided Solved Dataset 1 probes, faceted by the distractor impression type, mated impression type, and whether probe EFS data was provided

7 Michigan State Police

The results of Section 7 are based on searches of the sequestered dataset *Michigan State Police*. This dataset consist of of 2 239 operational latent probes. No EFS data was provided for probes or mated exemplars. All probes searched were a single friction ridge sample from somewhere on the hand.

Note: While NIST biometric technology evaluations typically use sequestered law enforcement data, a literature search indicates that this collection of data may have been supplied to other research organizations that are not subject to the same strict sequestration policies as NIST.

7.1 Failures

Table 15 shows the number of failures to create templates. Table 16 shows the number of failures to produce a candidate list.

Table 15: Number of failures to create templates.

Image Type	Content	Distal Failures	Palm Failures	Attempts
Exemplar	Image	2	0	1 367
Probe	Image	100	8	2 239

Table 16: Number of failures to produce a candidate list. This number includes any failures to create a probe template from Table 15.

Distractor Imp.	Probe Content	Distal Failures	Palm Failures	Attempts
Plain	Image	100	8	2 239
Roll	Image	100	8	2 239

7.2 CMC Plots

The CMC plots in Figure 10 show the FNIR of griaule+1006 when searching Michigan State Police against enrollment database where a single mated identity for each search probe was present. The plots are faceted by the distractor impression type. Tabular versions of FNIR at select ranks can be viewed in Table 17.

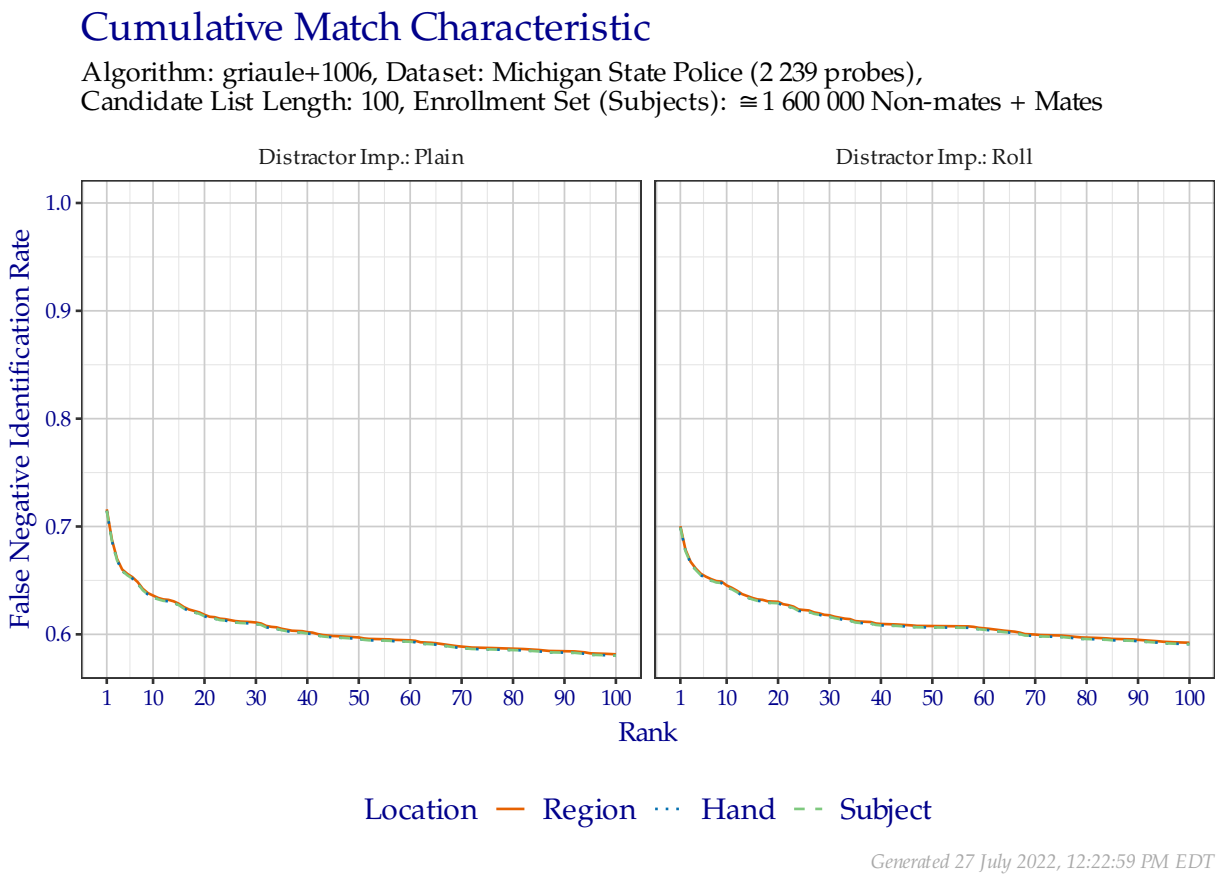

Figure 10: CMC when searching Michigan State Police probes, faceted by distractor impression type.

7.3 CMC Table

The values in Table 17 correspond to Figure 10.

Table 17: Region FNIR values from CMC plotted in Figure 10.

Distractor Imp.	Probe Content	Rank 1	Rank ≤ 50	Rank ≤ 100
Plain	Image	0.7159	0.5971	0.5815
Roll	Image	0.7003	0.6079	0.5922

7.4 Effect of Distal Region on CMC

The CMC in Figure 11 shows results from *only* the distal phalanx probes from Michigan State Police.

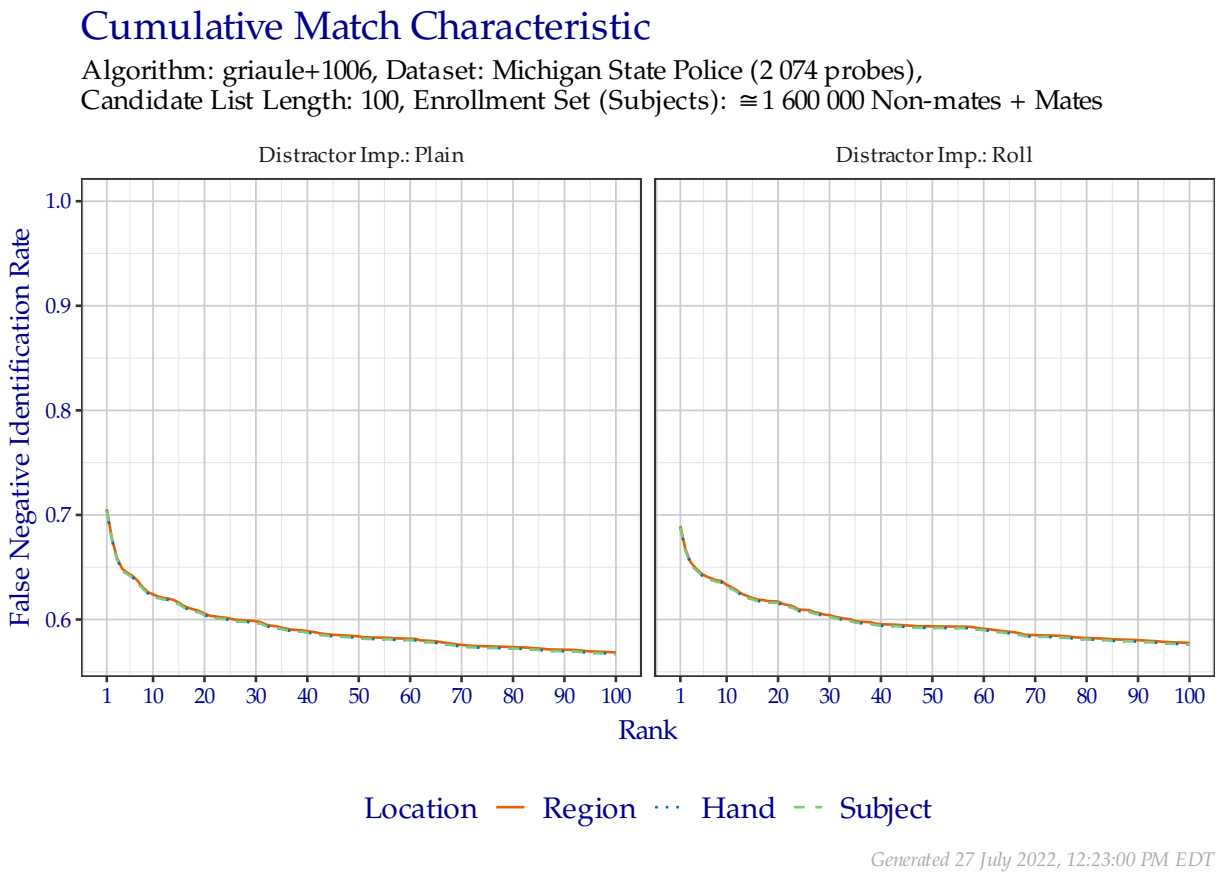

Figure 11: CMC when searching Michigan State Police distal phalanx probes, faceted by distractor impression type.

The values in Table 18 correspond to Figure 11.

Table 18: Region FNIR values corresponding to FPIR plotted in Figure 11.

Distractor Imp.	Probe Content	Rank 1	Rank ≤ 50	Rank ≤ 100
Plain	Image	0.7054	0.5839	0.5685
Roll	Image	0.6895	0.5935	0.5776

7.5 Effect of Palm Region on CMC

The CMC in Figure 12 shows results from *only* the palm probes from Michigan State Police.

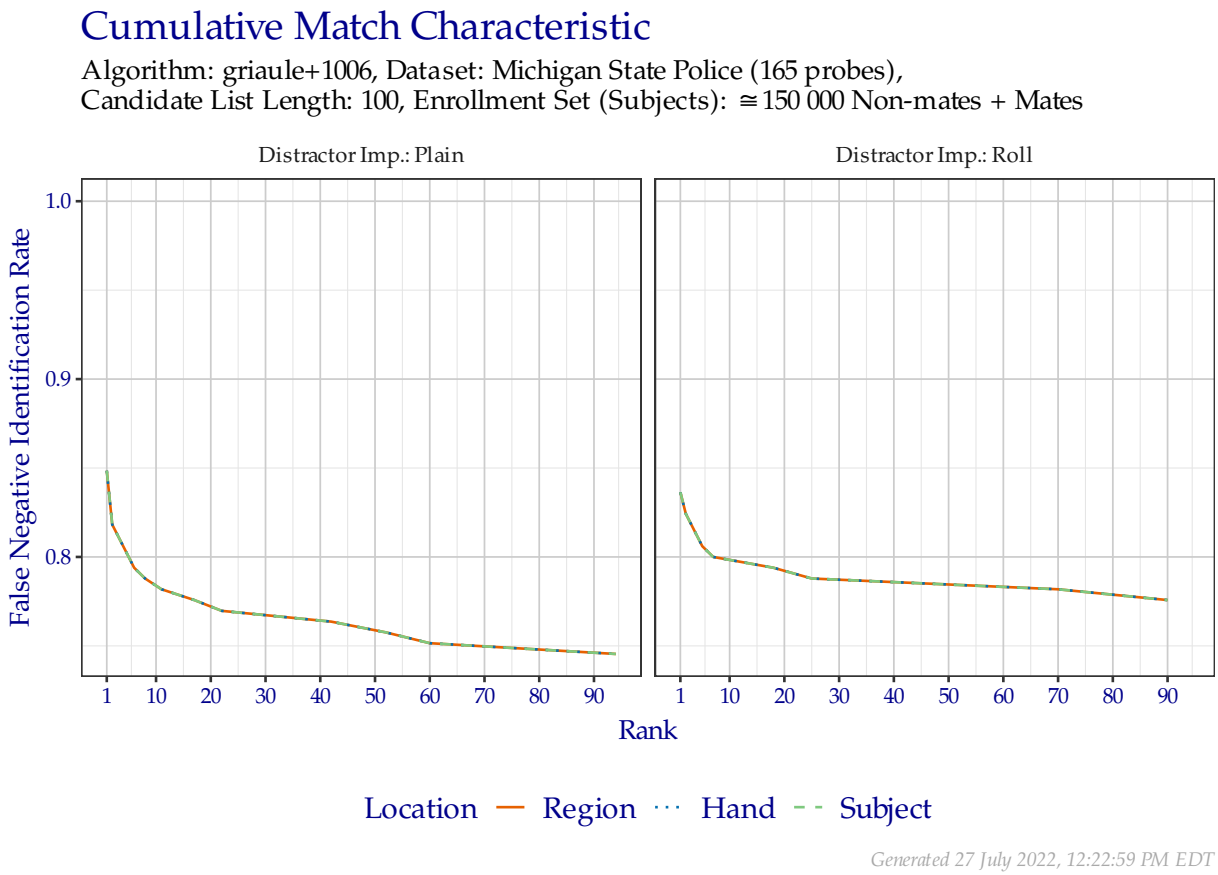

Figure 12: CMC when searching Michigan State Police palm probes, faceted by distractor impression type.

The values in Table 19 correspond to Figure 12.

Table 19: Region FNIR values corresponding to FPIR plotted in Figure 12.

Distractor Imp.	Probe Content	Rank 1	Rank ≤ 50	Rank ≤ 100
Plain	Image	0.8485	0.7636	0.7455
Roll	Image	0.8364	0.7879	0.7758

7.6 DET Plots

The DET plots in Figure 13 show the false positive and false negative identification rate tradeoffs of griaule+1006 when searching Michigan State Police against enrollment database where a single mated identity for each search probe was present. The plots are faceted by the distractor impression type. Tabular versions of FNIR at select FPIR can be viewed in Table 20.

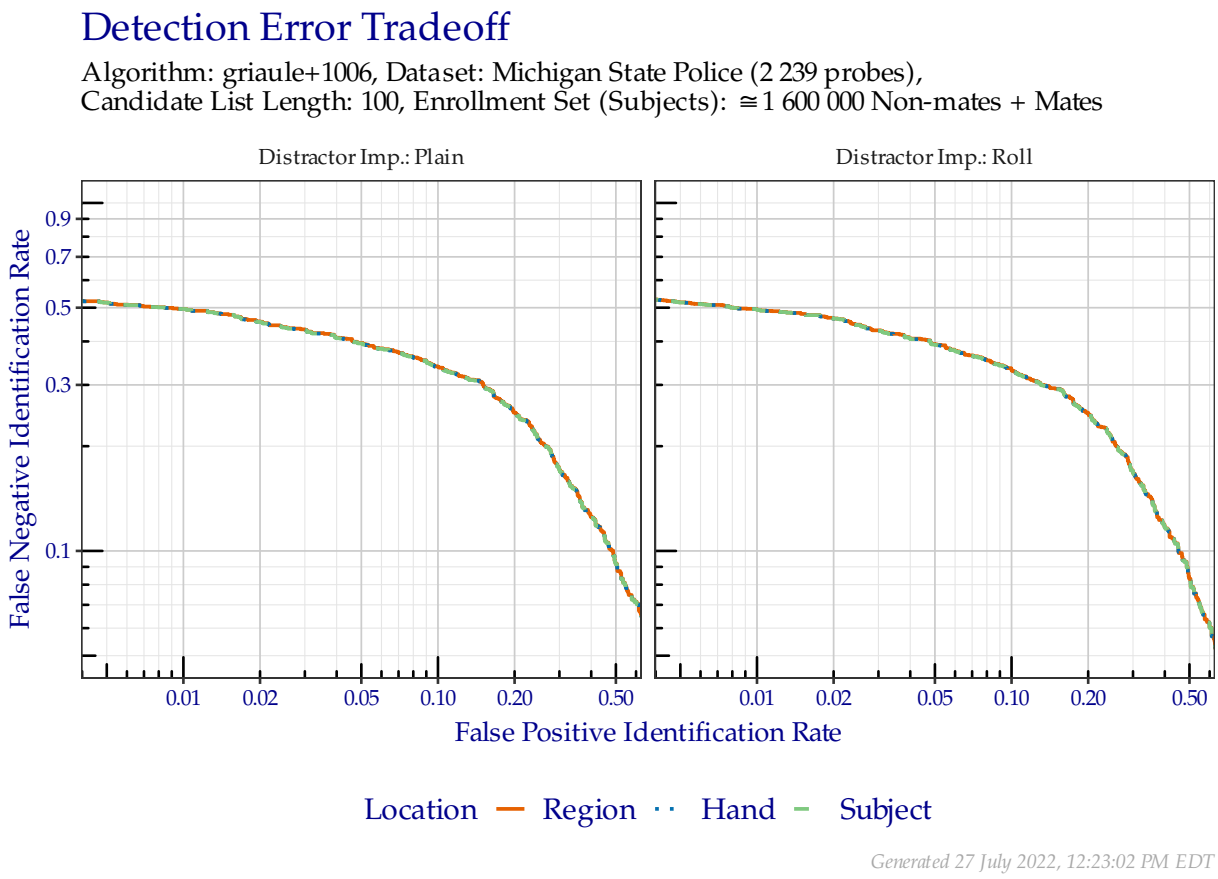

Figure 13: DET when searching Michigan State Police probes, faceted by the distractor impression type.

7.7 DET Table

The values in Table 20 correspond to Figure 13.

Table 20: Region FNIR values corresponding to FPIR plotted in Figure 13.

Distractor Imp.	Probe Content	FPIR = 0.01	FPIR = 0.02	FPIR = 0.1
Plain	Image	0.4963	0.4557	0.3383
Roll	Image	0.4940	0.4655	0.3308

7.8 Effect of Distal Region on DET

The DET in Figure 14 shows results from *only* the distal phalanx probes from Michigan State Police.

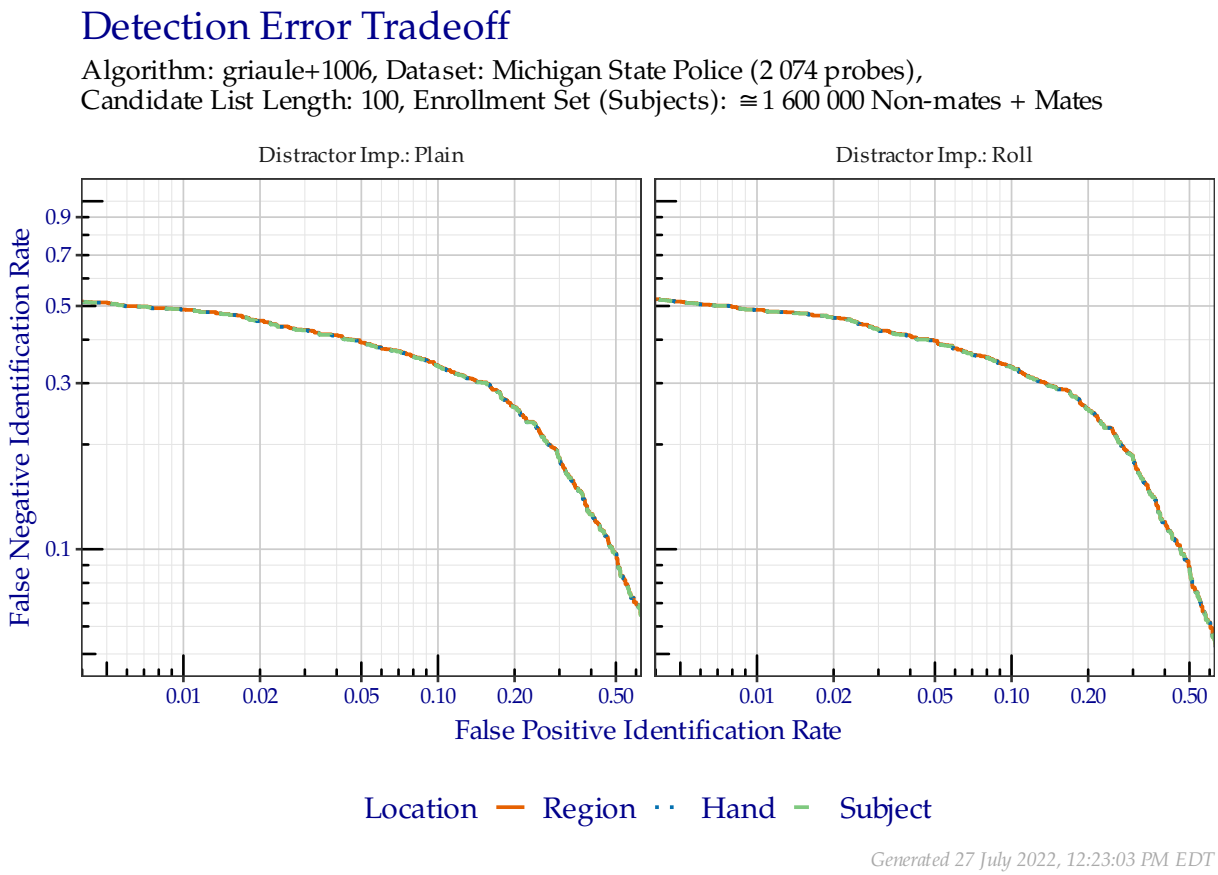

Figure 14: DET when searching Michigan State Police distal phalanx probes, faceted by distractor impression type.

The values in Table 21 correspond to Figure 14.

Table 21: Region FNIR values corresponding to FPIR plotted in Figure 14.

Distractor Imp.	Probe Content	FPIR = 0.01	FPIR = 0.02	FPIR = 0.1
Plain	Image	0.4883	0.4536	0.3374
Roll	Image	0.4874	0.4623	0.3345

7.9 Effect of Palm Region on DET

The DET in Figure 15 shows results from *only* the palm probes from Michigan State Police.

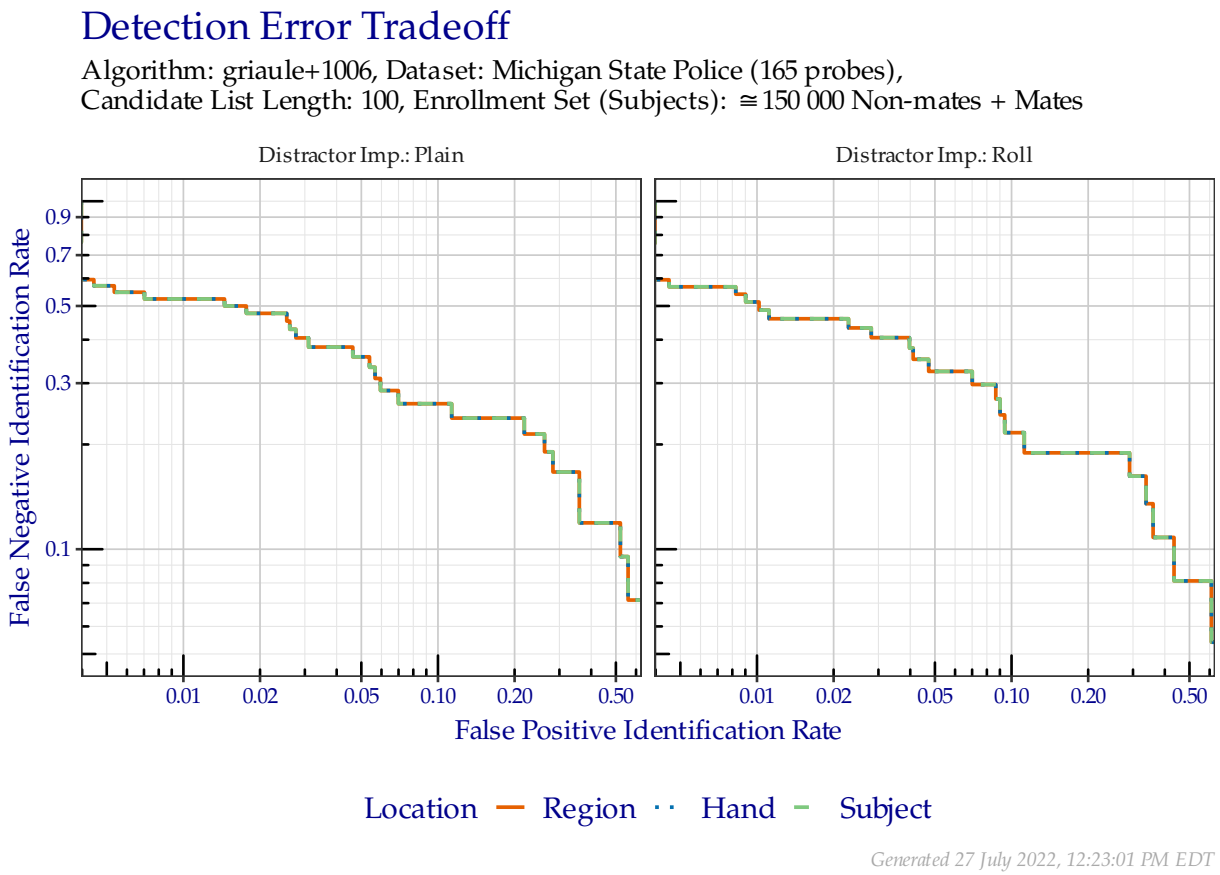

Figure 15: DET when searching Michigan State Police palm probes, faceted by distractor impression type.

The values in Table 22 correspond to Figure 15.

Table 22: Region FNIR values corresponding to FPIR plotted in Figure 15.

Distractor Imp.	Probe Content	FPIR = 0.01	FPIR = 0.02	FPIR = 0.1
Plain	Image	0.5238	0.4762	0.2619
Roll	Image	0.5135	0.4595	0.2162